## **Commissioning of Soft X-ray Nanoscopy Beamline at the Taiwan Photon Source**

Commissioning of a soft X-ray nanoscopy beamline at the Taiwan Photon Source 27A (**TPS 27A**) is currently underway. Powered by an elliptically polarized undulator, EPU66, and a newly designed active-mirror plane-grating monochromator (AMPGM), the **TPS 27A** beamline is capable of delivering a photon beam with high energy-resolving power at a constant beam size. Here, we report the commissioning status of beamline **TPS 27A** and its two microscopy endstations: the scanning transmission X-ray microscope (STXM) and photoelectron microscope (photoelectron-related imaging and nano-spectroscopy, PRINS). The STXM endstation is partially opened to users as of the end of 2024, and the PRINS endstation is expected to reach the same status by late 2025.

I. Beamline TPS 27A and 27A1 STXM Endstation

The **TPS 27A** Soft Nanoscopy beamline is designed to deliver a high resolving power and photon flux across a broad photon energy range. To achieve this, a specially developed in-house AMPGM monochromator system with three plane gratings has been implemented. This design supports an energy range from 90 to 3000 eV, with the three gratings covering specific subranges: 90–320 eV, 280–1060 eV, and 1000-3000 eV. Additionally, with the EPU66 undulator system, the photon polarization can be tuned to horizontal, vertical, left-circular, and right-circular states. The beamline is currently in the commissioning stage, which is conducted at the TPS 27A1 STXM endstation. The first X-ray absorption spectroscopy (XAS) of nitrogen gas has been successfully demonstrated, as shown in Fig. 1. The nitrogen K-edge absorption spectroscopy results reveal five distinct vibrational levels in the N1s  $\rightarrow 1\pi_g^*$ transition. Fitting analysis indicates that the full width at half maximum (FWHM) for Gaussian and Lorentzian components are 32 and 110 meV,

respectively. This corresponds to a resolving power of 12,500 at 400 eV, which aligns well with the expected performance. Currently, the commissioning of the 280–1060 eV energy range is nearly complete. Testing for the 90–320 eV range is planned for the first half of 2025, followed by the testing of the 1000–3000 eV range in the second half of the year.

The **TPS 27A1** endstation is designed to perform XAS-related chemical mapping in transmission mode. Its core components include the Zone Plate (ZP) and scanning stages. The STXM endstation is equipped with multiple scanning systems, including stepping motors, piezo walking stages, and piezo actuators with a laser interferometer feedback system. These systems together maintain the relative position between the ZP and the sample, ensuring nanometer-level positioning performance during energy changes and scans, as illustrated in **Fig. 2**. Due to the fundamental properties of ZPs, where the focal length is proportional to the photon energy, the system is carefully designed and fine-tuned to maintain the imaging area with less than 1  $\mu$ m lateral movement across the photon energy range of 280–1060 eV.

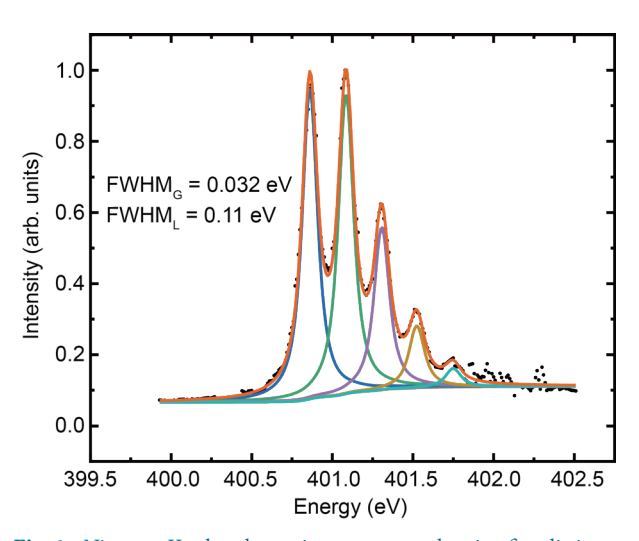


Fig. 1: Nitrogen K-edge absorption spectrum, showing five distinct vibrational levels in the N1s  $\rightarrow$  1 $\pi_g^+$  transition. The fitted curve highlights the high-resolution capability of the beamline.

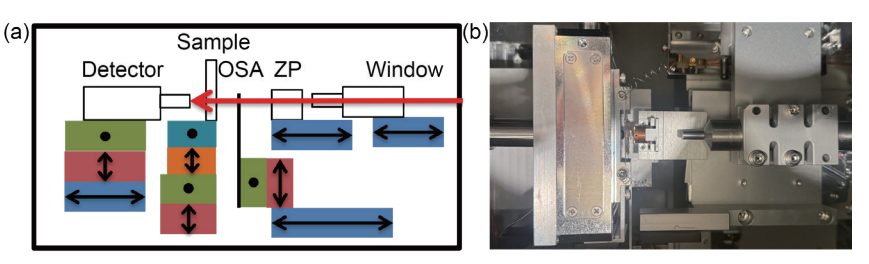


Fig. 2: (a) Schematic representation of the STXM endstation, illustrating the multiple scanning stages, including stepping motors, piezo walking stages, and piezo actuators. (b) Top-view photograph of the STXM endstation, showing the physical layout of the ZP and scanning stages. These components function together to maintain nanometer-level positioning accuracy during energy changes and scans.

Chemical mapping using the spectroscopy capabilities of the STXM endstation is illustrated in Fig. 3. The sample consists of Cu nanoparticles (NPs) doped into g-C<sub>3</sub>N<sub>4</sub>. The STXM elemental mapping, as presented in Fig. 3(a), was conducted at the Cu L-edge and N K-edge. The green region corresponds to the nitrogen signal, while the red region represents the copper signal. These signals were obtained by calculating the difference between the  $\pi^*$  C-N-C peak and the pre-edge for nitrogen, and the Cu main peak and the pre-edge for copper. The corresponding spectra from the Cu L-edge and N K-edge are shown in Figs. 3(b) and 3(c), respectively. The spectrum shown in Fig. 3(b) was acquired from the red regions in the elemental map, which highlight the copper signal. Similarly, the spectrum in Fig. 3(c) was obtained from the green regions, which represent the nitrogen signal. These results demonstrate the powerful capabilities of STXM in combining highresolution microscopy with detailed spectroscopic analysis.

This year, the STXM endstation successfully achieved its first light, marking a significant milestone in its development. Through the current data and commissioning results, we have successfully demonstrated the powerful capabilities of the STXM endstation in delivering highquality nanoscale imaging and chemical mapping. These achievements validate the endstation's readiness to support the advanced research across diverse scientific fields. This cutting-edge STXM endstation is the result of a collaborative effort between the Department of Physics at Tamkang University and the NSRRC, exemplifying the strength of cross-institutional collaboration in driving scientific innovation. To celebrate this milestone, the Opening Ceremony for the TPS 27A1 Nanoscopy Beamline and STXM Endstation was held in late December 2024. Moving forward, commissioning efforts will continue in 2025 to further expand the operational energy range and enable more advanced experimental methodologies.

## II. TPS 27A2 PRINS Endstation

The **TPS 27A2** endstation aims to perform photoelectronrelated imaging and nano-spectroscopy, and its core is

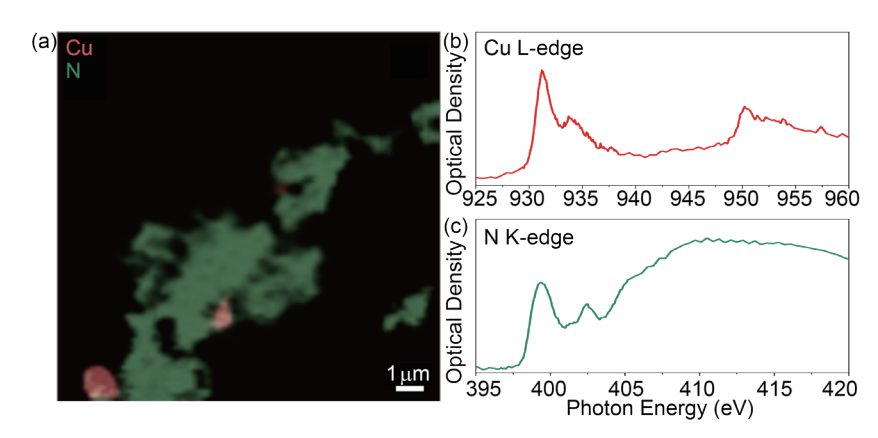
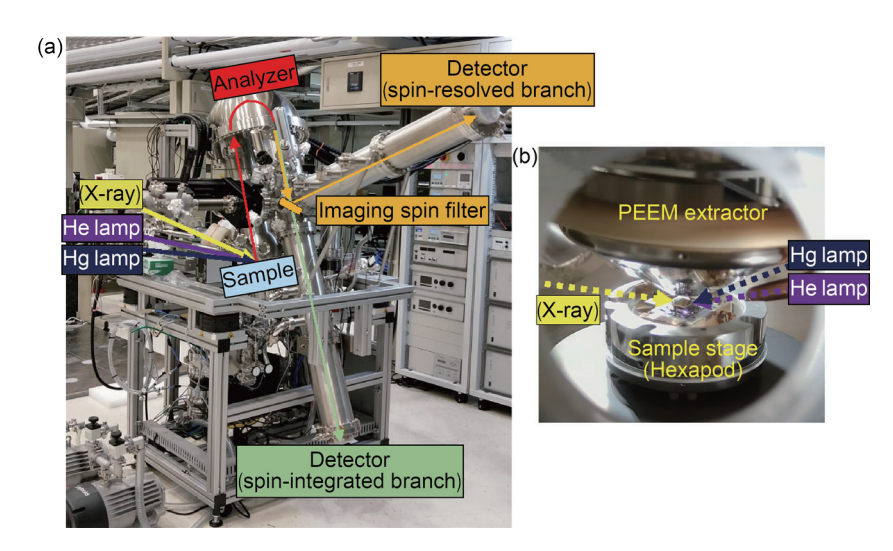


Fig. 3: (a) Elemental mapping of Fe and N for Cu NP/g- $C_3N_4$ . (b,c) Corresponding XAS spectra obtained from the red and green regions, respectively.



**Fig. 4**: (a) Configuration of the photoelectron microscope system at the **TPS 27A2**. The beam paths of photoelectrons are indicated by green arrows for the spin-integrated branch or by orange ones for the spin-resolved branch. (b) Image taken close to the hexapod sample stage, extractor lens, and the capillary of the helium discharge lamp. [Reproduced from Ref. 2]

a photoelectron momentum microscope (MM) system, which is capable of obtaining direct-space imaging, momentum-space imaging, and photoelectron spectroscopy with position sensitivity. The off-line commissioning utilizing both ultraviolet (UV) He discharge lamp and Hg arc lamp has been initiated from mid-2022, and the off-line commissioning results have been reported in early 2024.

The MM system configuration is shown in **Fig. 4**. All light sources, including the soft X-rays and UV lamps, are incident at an angle of 22° relative to the sample surface. The excited photoelectrons are extracted by the extractor lens and projected onto 2D detectors either along the spin-integrated branch or the spin-resolved branch when an imaging spin filter is introduced.

The spatial resolution of direct-space images was tested by analyzing the intensity profile measured on a standard checkerboard-patterned specimen illuminated by the Hg lamp, and the results are shown in **Fig. 5**. The largest field of view (FoV) is approximately 700  $\mu$ m (**Fig. 5(a)**), and the

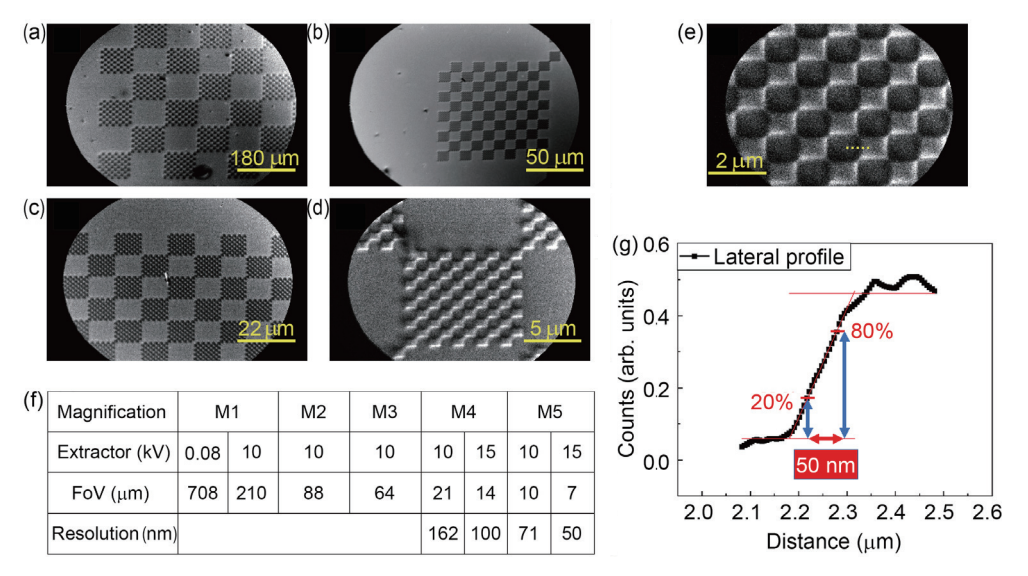


Fig. 5: (a–e) Direct-space photoelectron images of a checkerboard-patterned sample with different FoVs illuminated by the Hg lamp. (f) Table of imaging magnification settings, corresponding FoVs, and resolution. (g) Intensity profile along the edge of the Au patterns marked as a dashed line in (e). [Reproduced from Ref. 2]

smallest FoV is approximately 7  $\mu$ m (**Fig. 5(e)**). Various magnification settings and the corresponding FoVs are listed in the table of **Fig. 5(f)**. The spatial resolution was estimated to be 50 nm by analyzing the intensity profile shown in **Fig. 5(g)** along the edge of the Au patterns, as indicated by a dashed line in **Fig. 5(e)**.

The momentum-space imaging was tested on a Au(111) single-crystal surface by He(I) radiation (21.2 eV), and the results are summarized in **Fig. 6**. A series of momentum-space images exceeding the first Brillouin zone taken at different binding energies are recorded and shown in **Fig. 6(a)**. After stacking all constant-energy contours together to construct a 3D dataset ( $k_x$ ,  $k_y$ ,  $E_B$ ), which is shown in **Fig. 6(b)**, the electronic band structure along any high-symmetry directions can be obtained simultaneously.

In early 2025, more capabilities can be explored using soft X-rays covered by the **TPS 27A** beamline, including the imaging based on XAS, X-ray photoelectron spectroscopy, and X-ray magnetic circular/linear dichroism, which can provide additional element-resolved and magnetization-resolved information. (Reported by Hung-Wei Shiu and Tzu-Hung Chuang)

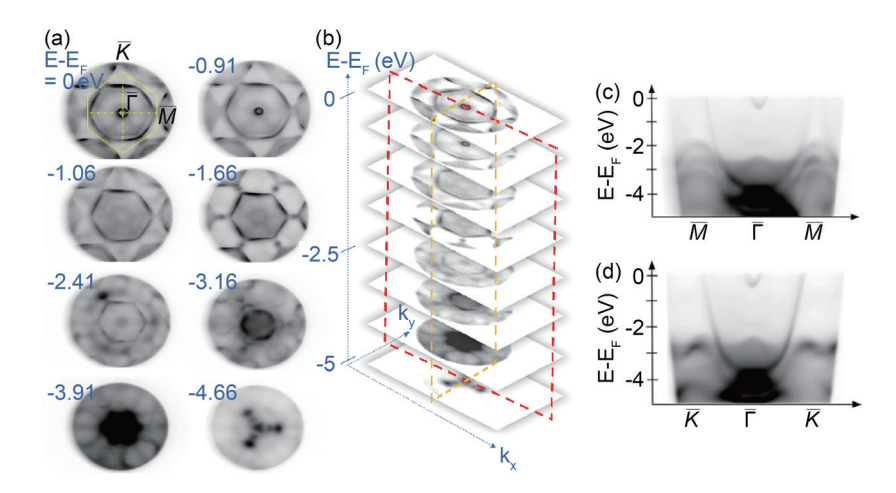


Fig. 6: (a) Momentum-space images recorded at different binding energies obtained from a Au(111) surface at 300 K illuminated by He(I) radiation. (b) Stacking of a series of momentum images with various binding energies, forming a 3D dataset of ( $k_x$ ,  $k_y$ ,  $E_B$ ). (c,d) Slice of the 3D dataset along high-symmetry points of M-Γ-M and K- Γ-K, respectively. [Reproduced from Ref. 2]

## References

- H.-W. Shiu, T.-H. Chuang, C.-M. Cheng, C.-H. Chen, Y.-J. Hsu, D.-H. Wei, J. Electron Spectrosc. Relat. Phenom. 266, 147363 (2023).
- 2. T.-H. Chuang, C.-C. Hsu, W.-S. Chiu, J.-S. Jhuang, I-C. Yeh, R.-S. Chen, S. Gwo, D.-H. Wei, J. Synchrotron Rad. **31**, 195 (2024).